Controlling Toroidal Moment by Means of an Inhomogeneous Static Field: An *Ab Initio* Study

S. Prosandeev,[1,2] I. Ponomareva,[1] I. Kornev,[1] I. Naumov,[1] and L. Bellaiche[1]
[1]*Physics Department, University of Arkansas, Fayetteville, Arkansas 72701, USA*
[2]*Rostov State University, Rostov on Don, 344090, Russia*
(Received 9 February 2006; revised manuscript received 6 April 2006; published 16 June 2006)

A first-principles-based approach is used to show (i) that stress-free ferroelectric nanodots under open-circuit-like electrical boundary conditions maintain a vortex structure for their local dipoles when subject to a transverse inhomogeneous static electric field, and, more importantly, (ii) that such a field leads to the solution of a fundamental and technological challenge: namely, the efficient control of the direction of the macroscopic toroidal moment. The effects responsible for such striking features are revealed and discussed.

DOI: 10.1103/PhysRevLett.96.237601 PACS numbers: 77.80.Bh, 77.22.Ej, 77.84.Dy

The unique properties of ferroelectric and ferromagnetic solids are widely used in many important applications. Interestingly, these properties can dramatically change when going from bulks to nanostructures [1–3]. For instance, it has been recently discovered that zero-dimensional (0D) ferroelectrics can have a vortex structure for their dipoles below a critical temperature [4,5]. Such an unusual vortex resembles the curling state exhibited by magnetic dots above a certain size [1,6] and leads to the activation of a macroscopic toroidal moment, which involves the cross product between the $\mathbf{r}_i$ vectors locating the i unit cells and their local electrical dipoles $\mathbf{p}_i$, i.e., it is defined as $\mathbf{G} = \frac{1}{2N}\sum_i \mathbf{r}_i \times \mathbf{p}_i$, where the sum runs over the N unit cells of the 0D system.

The possibility of switching the direction of the toroidal moment opens exciting opportunities for nanomemory devices [4,7], nanomotors, nanotransducers, nanoswitchers, nanosensors, etc. However, a practical control of the $\mathbf{G}$ toroidal moment is rather challenging, mostly due to the fact that electric toroids directly interact with the *curl* of $\mathbf{E}$ but not with an uniform electric field alone [8]. Moreover, a nonvanishing *curl* of $\mathbf{E}$ can *only* be produced (according to Maxwell equations) by a temporal change of the magnetic field, $-d\mathbf{B}/dt$, but the magnitude of the magnetic field necessary to switch the electric toroidal moment is impractical. Furthermore, even if this large magnetic field was reachable, it would disturb a volume of the sample much larger than the nanodot size. As a result, manipulating the toroidal moment of a *single* nanodot, separately from the toroidal moment of the other dots of the sample, will become impossible—which will thus seriously limit the benefits of using toroids for creating the next generation of ''wunderbar'' devices. (One also needs to be able to ''read'' the chirality of the vortex of a single nanodot via, e.g., the field produced by its dipoles [4].)

The aims of this Letter is twofold: (1) to report first-principles-based simulations demonstrating that there is an original and efficient way to control the electric toroidal moment of a single nanodot, namely, by using an inhomogeneous static electric field; and (2) to reveal, and understand, the reasons for such control.

Here, we use the first-principles-based Monte Carlo scheme of Ref. [9] to study a $12 \times 12 \times 12$ stress-free cubic dot that is under open-circuit electrical boundary conditions and that is made of $Pb(Zr_{0.4}Ti_{0.6})O_3$ (PZT)—with the surfaces being Pb-O terminated. This scheme generalizes to 0D systems the alloy effective Hamiltonian method proposed in Ref. [10] for bulks, by (i) substituting the dipole-dipole interaction of infinite three-dimensional systems by the corresponding interaction in 0D materials [5]; and (ii) incorporating surface-induced atomic relaxations that are caused by the vacuum surrounding the dot—with the governing parameters having been fitted to first-principles calculations on Pb-O terminated PZT thin films [11]. We consider a transverse inhomogeneous electric field arising from charges located away from the studied dot, and incorporate the interaction between the dipoles in the dot and this field in the total energy provided by the effective Hamiltonian method. The temperature is decreased by small steps, and the x, y, and z axis are chosen along the pseudocubic [100], [010], and [001] directions, respectively.

Figure 1 shows the two setups that we considered, as well as the resulting inhomogeneous field and ground-state dipole pattern in the dot. In practice, such setups and inhomogeneous fields can be generated by, e.g., piezoforce-microscopy tip(s), nanowires, switching ferroelectric dots, or other original methods.

Let us first discuss the setup of Fig. 1(a). The dipolar source of the field is made of two opposite charges of 2×10^{-17} C distant of 15 primitive unit cells along the x axis from the center of the investigated dot—resulting in a field magnitude of about 2×10^8 V/m in the center of this dot. One interesting result of Fig. 1(a) is that the studied dot under this inhomogeneous field maintains a vortex structure at low temperature. The interactions between the dipoles of the dot under open-circuit conditions and the inhomogeneous field are thus not strong enough to overcome the depolarizing-field effects responsible for the existence of a toroidal moment in an isolated dot [4,5] [One can, in fact, ''break'' this vortex structure by applying fields with magnitude several times larger than the one

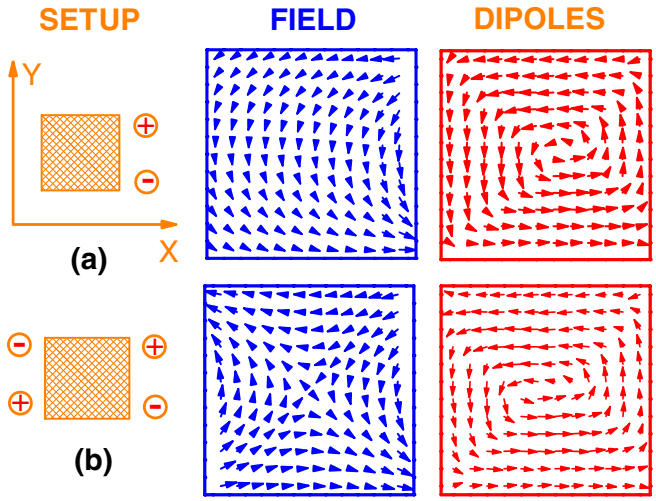

FIG. 1 (color online). Schematization of the two setups considered in this study, the resulting inhomogeneous electric fields at the sites of the dot, and the ground-state dipole pattern.

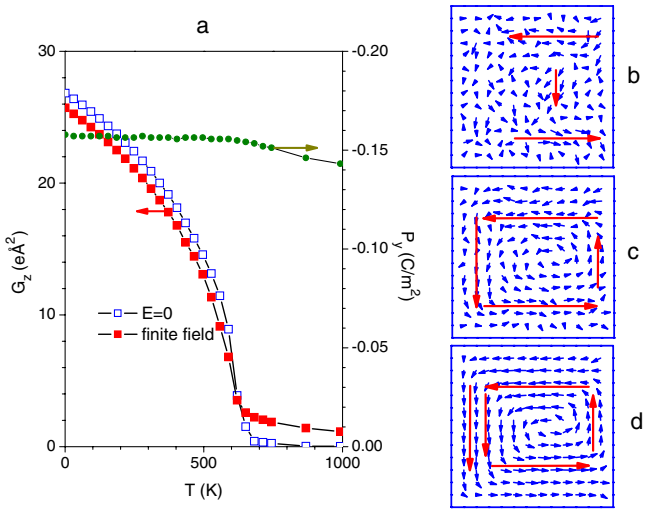

FIG. 2 (color online). (a) Temperature dependency of the toroidal moment (squares) and polarization (dots) in the setup shown in Fig. 1(a); and (b–d) resulting dipole pattern at 625, 300, and 1 K, respectively. The filled symbols of panel (a) correspond to simulations in which the inhomogeneous field is turned on while open symbols show results for an isolated dot (that is a dot under no field, and which does not exhibit any polarization). The long and thick arrows of panels (b–d) are guides for the eyes to show the tendency of some dipoles to align along some specific directions. The temperature has been rescaled, as in Ref. [10], to fit the experimental value of the Curie temperature of $Pb(Zr_{0.5}Ti_{0.5})O_3$ solid solution.

shown in Fig. 1(a), but such huge fields are unrealistic]. Figure 1(a) also reveals that dipoles located at the left side of the dot, as well as those located at the bottom and top of the dot, are following in overall the inhomogeneous field. On the other hand, at the right side of the dot, some dipoles are directed *against* this field despite the fact that the field is rather strong there. Fighting against these strong fields results in dipoles smaller in magnitude at the right side of the dot than those at the left side of the dot. This leads to the appearance of a spontaneous polarization along the $-y$ axis—while the toroidal moment is along the $+z$ axis. In other words and unlike in the isolated dot (that is in the dot under no field) [4], toroidal moment and polarization coexist in the dot under the inhomogeneous field associated with the first setup. (This polarization is weak, namely 0.158 C/m^2 to be compared with the polarization of $\simeq$1 C/m^2 for bulk PZT.) As we will see later, the understanding of the dipole arrangement of Fig. 1(a) is the key to allow an efficient control of the toroidal moment's direction.

Figure 2(a) displays the *temperature* dependency of **G**—computed with respect to the dot center—switching *on and off* the field of Fig. 1(a). This inhomogeneous field has two rather weak-in-magnitude effects on **G**, namely, it makes the toroidal moment slightly smaller at low temperature and results in a high-temperature tail—which is reminiscent of the polarization tail exhibited by ferroelectric bulks subject to an homogeneous electric field. Note, however, that the toroidal moment of the ground state in the isolated dot can be along any of the six $\langle 001 \rangle$ directions while its direction is *unique* when the inhomogeneous field is turned on. Figure 2 also displays the temperature dependency of the spontaneous polarization in the dot experiencing the conditions associated with the first setup. Our simulations reveal that this polarization exists at the highest considered temperatures and is mostly independent of temperature below $\simeq$ 600 K. This weak polarization is thus solely caused by the field rather than the (temperature-dependent) polarization instability.

The resulting change of the dipole pattern with temperature is shown in Figs. 2(b)–2(d). At high temperatures, dipoles *located at the top and bottom parts of the dot along the y axis* follow the inhomogeneous field displayed in Fig. 1(a). They thus preferentially align in opposite directions along the x axis. A plane-by-plane decomposition of **G** (not shown here) undoubtedly indicates that these *antiphase chains are responsible for the high-temperature tail of* **G** seen in Fig. 2(a). Furthermore, the dipoles located *outside* these chains have a slight tendency to exhibit a component along $-y$. This results in the weak polarization. Figures 2(b)–2(d) further show that these antiphase chains elongate along the x axis with their dipoles becoming bigger in magnitude as temperature is decreased. These antiphase chains constitute a nucleus for **G** to develop by forcing the dipoles in the other parts of the dot to change their directions as temperature decreases, in order to generate a "full" vortex (which provides the lowest electrostatic energy). Some dipoles on the left and right sides of the dot are thus now antiparallel and parallel to the y axis, respectively, and all increase in magnitude as the temperature is decreased—which explains why **G** significantly

increases when decreasing the temperature, see Fig. 2(a). The direction of **G** is thus determined by the antiphase chains of dipoles located at the top and bottom of the dot, and resulting from following the inhomogeneous field there. Such effect implies that *rotating* the source of the inhomogeneous field should affect the direction of **G**. Such possible control of the toroidal moment is indeed confirmed by Fig. 3, which shows the computed dependency of the toroidal moment (and polarization) on the Θ angle of the rotation about the x axis of the dipolar source in the setup schematized in Fig. 1(a). For instance, reversing the source of the inhomogeneous field (that is, when Θ is varied from 0 to 180°) leads to **G**, which is now antiparallel rather than parallel to the z axis—as well as a polarization that is now parallel to the y axis. Figure 3 further indicates that the toroidal moment nearly abruptly changes direction by 90° for Θ equal to 45°, 135°, 225°, and 315°, while the (weak) polarization is a smooth function of Θ. Such behavior indicates that the six $\langle 001 \rangle$ minima of **G** are not flat and have 90°-energy barriers that are smaller than their 180°-energy barriers.

We now wonder if some particular inhomogeneous fields can lead to a toroidal moment that can still be controlled but that does *not* coexist with any polarization. (A polarization can hinder the benefits of having torroidal moments for future applications because polarizations, unlike toroidal moments, of different dots would interact strongly [4].) The setup of Fig. 1(b) is an example of how to achieve that, and consists in symmetrically placing two

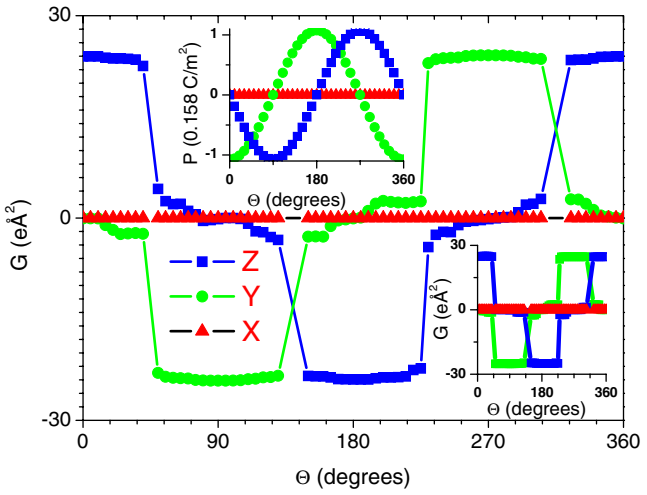

FIG. 3 (color online). Dependency of the Cartesian components of the ground-state toroidal moment and polarization (in the top inset) on the angle of rotation about the x axis of the dipolar source associated with the setup of Fig. 1(a). For each angle, the calculations are first performed at high temperature and then slowly cooled down until 1 K. The bottom inset reports the dependency of the ground-state toroidal moment for the setup of Fig. 1(b) (for which no polarization exists) with respect to the angle of rotation about the x axis of the two dipolar sources.

opposite dipolar sources at the left and right sides of the studied dot, respectively. Note, in particular, that (i) the fields are now equally strong at the left *and* right sides of the dot; and (ii) the antiphase chains of dipoles still occurring at the bottom and top y regions of the dot are now forcing some dipoles in the right *and* left sides of the dots to *lie against* these fields in order to create a full vortex [see Fig. 1(b)]. The bottom inset of Fig. 3 also shows that the toroidal moment can indeed be controlled for the setup displayed in Fig. 1(b) by playing with the orientation of the dipolar sources. In particular, the simultaneous reversal of the two sources of Fig. 1(b) results in a toroidal moment switching its direction from $+z$ to $-z$ (without creating any polarization).

Let us now understand why the second setup does not produce any polarization, and why we numerically find (not shown here) that an *homogeneous* field is *unable* to control the toroidal moment's *direction* in the dot while generating a nonzero polarization. For that, it is enough to consider the linear response of the $\mathbf{p}_i(\mathbf{E}_i)$ dipole at the site i with respect to the $\mathbf{E}_i$ field located at this site: i.e., $\mathbf{p}_i(\mathbf{E}_i) = \mathbf{p}_i(0) + \gamma \mathbf{E}_i$, where $\mathbf{p}_i(0)$ is the dipole at site i in the isolated dot (i.e., when no field is turned on) and γ is the polarizability. It is straightforward [when summing over all the sites i and recalling that the isolated dot has a nonvanishing $\mathbf{G}(0)$ toroidal moment but a null polarization] to prove that this equation results in a **P** polarization and **G** toroid moment such as

$$\mathbf{P} \propto \gamma \sum_i \mathbf{E}_i \quad \text{and} \quad [\mathbf{G} - \mathbf{G}(0)] \propto \gamma \sum_i \mathbf{r}_i \times \mathbf{E}_i, \qquad (1)$$

where the $\mathbf{r}_i$ vectors locate the i unit cells with respect to the dot center. The first equation implies that applying any *homogeneous* field, as well as the nonsymmetrical inhomogeneous field of the first setup [see Fig. 1(a)], leads to a nonzero polarization, unlike in the case of the more symmetrical inhomogeneous field of the second setup [for which $\sum_i \mathbf{E}_i$ is null, see Fig. 1(b)]. The right part of the second equation vanishes for an homogeneous electric field (because $\sum_i \mathbf{r}_i$ is null for the considered cubic structure), while we numerically find that it is *not* the case for the inhomogeneous fields considered here. Considering nonlinear terms in $\mathbf{E}_i$ for $\mathbf{p}_i(\mathbf{E}_i)$ leads to the same conclusions.

Moreover, the qualitative control of the direction of **G** by inhomogeneous electric fields is a general feature of 0D ferroelectrics, since we found it (not shown here) to be independent of the surface termination (we checked that by switching off the parameters related to surface termination) and of the shape of the dot (we confirmed that by investigating spheres, cubes, discs, cylinders, and asymmetrically-cut pyramids). Furthermore, additional calculations for which we allow a 50% screening of the surface-charges—that is a realistic electrical boundary conditions [12], and for which we still have a vortex structure for the isolated dot [5]—also yield such control.

Let us now discuss differences or analogies between magnetic and electrical vortices. First of all, the nearest-neighbor exchange interactions are much stronger than the dipole-dipole interactions in magnetic systems, which results in a *magnetized* core of the vortex [1,13] and requires relatively *large* sizes of the nanodots to have a vortex structure. In contrast, because of the large depolarizing energy, very *small* ferroelectric dots [4,5] can have a vortex structure *without any polarization*. These constitute strong advantages of ferroelectric dots over magnetic dots for increasing memory capabilities [4]—via the control of **G** of *single* dots by, e.g., the setup of Fig. 1(b). [Notice that in this setup, the electric vortex produces a local field, which can be put in use for sensing and writing]. Second, the electric toroidal moment **G**, being a cross product of two vectors, is an axial vector, and, consequently, does not break the space symmetry. It also does not break the time symmetry—unlike the magnetic toroidal moment $\mathbf{T} = \frac{1}{2N}\sum_i \mathbf{r}_i \times \mathbf{m}_i$, where $\mathbf{m_i}$ are the local magnetic dipoles at the N lattice sites, which breaks both the time and space symmetry [8,14–16]. As a result, our main finding that inhomogeneous electric fields (whose cross product with $\mathbf{r}_i$ does not break neither time nor space symmetry) can control **G** should imply, by symmetry arguments, that inhomogeneous *magnetic* fields (whose cross product with $\mathbf{r}_i$ breaks time and space symmetry) can switch the direction of **T**. Such analogy is consistent with the observed interactions of magnetic vortices with magnetic fields in *asymmetric* structures [17]—and thus exhibiting a similarity with the setup shown in Fig. 1(a).

In summary, first-principles-based simulations demonstrate that transverse inhomogeneous electric fields can control and switch the direction of the electric toroidal moment. Analysis of our calculations provides an understanding of the effects allowing such control and, in particular, points to the importance of the inhomogeneous-field-induced creation of antiphase chains.

We thank Huaxiang Fu for useful discussions. This work is mostly supported by DOE grant No. DE-FG02-05ER46188. We also acknowledge support from ONR Grant No. N00014-04-1-0413 and NSF Grant No. DMR-0404335. Some computations were made possible thanks to the MRI Grant No. 0421099 from NSF. S. P. also thanks RFBR Grants No. 01-02-629&94WFD0100021.

[1] S. D. Bader, Rev. Mod. Phys. **78**, 1 (2006).
[2] M. Dawber, I. Szafraniak, M. Alexe, and J. F. Scott, J. Phys. Condens. Matter **15**, L667 (2003).
[3] S. K. Streiffer, J. A. Eastman, D. D. Fong, C. Thompson, A. Munkholm, M. V. R. Murty, O. Auciello, G. R. Bai, and G. B. Stephenson, Phys. Rev. Lett. **89**, 067601 (2002).
[4] I. Naumov, L. Bellaiche, and H. Fu, Nature (London) **432**, 737 (2004).
[5] I. Ponomareva, I. I. Naumov, I. Kornev, Huaxiang Fu, and L. Bellaiche, Phys. Rev. B **72**, 140102(R) (2005); I. Ponomareva, I. I. Naumov, and L. Bellaiche, Phys. Rev. B **72**, 214118 (2005).
[6] A. Hubert and R. Schafer, *Magnetic domains* (Springer, New York, 2000), p. 167.
[7] V. M. Dubovik, M. A. Martsenyuk, and N. M. Martsenyuk, J. Magn. Magn. Mater. **145**, 211 (1995).
[8] V. M. Dubovik and V. V. Tugushev, Phys. Rep. **187**, 145 (1990).
[9] H. Fu and L. Bellaiche, Phys. Rev. Lett. **91**, 257601 (2003).
[10] L. Bellaiche, A. Garcia, and D. Vanderbilt, Phys. Rev. Lett. **84**, 5427 (2000).
[11] E. Almahmoud, Y. Navtsenya, I. Kornev, H. Fu, and L. Bellaiche, Phys. Rev. B **70**, 220102(R) (2004).
[12] J. Junquera and P. Ghosez, Nature (London) **422**, 506 (2003).
[13] K. Nakamura, T. Ito, and A. J. Freeman, Phys. Rev. B **68**, 180404(R) (2003).
[14] A. A. Gorbatsevich and Yu. Kopaev, Ferroelectrics **161**, 321 (1994).
[15] H. Schmid, Ferroelectrics **252**, 41 (2001).
[16] V. L. Ginzburg, Phys. Usp. **44**, 1037 (2001).
[17] M. Schneider, H. Hoffmann, and J. Zweck, Appl. Phys. Lett. **79**, 3113 (2001).